

## MINERALOGIC VARIABILITY OF THE KELSO DUNES, MOJAVE DESERT, CALIFORNIA DERIVED FROM THERMAL INFRARED MULTISPECTRAL SCANNER (TIMS) DATA

Michael S. Ramsey<sup>1</sup>, Douglas A. Howard<sup>1</sup>,  
Philip R. Christensen<sup>1</sup> and Nicholas Lancaster<sup>2</sup>

<sup>1</sup>Department of Geology  
Arizona State University  
Tempe, Arizona 85287-1404

<sup>2</sup>Desert Research Institute  
7010 Dandini Blvd.  
Reno, Nevada 89512

### 1. INTRODUCTION

Mineral identification and mapping of alluvial material using thermal infrared (TIR) remote sensing is extremely useful for tracking sediment transport, assessing the degree of weathering and locating sediment sources. As a result of the linear relation between a mineral's percentage in a given area (image pixel) and the depth of its diagnostic spectral features, TIR spectra can be deconvolved in order to ascertain mineralogic percentages (Ramsey and Christensen, 1992; Gillespie, et al., 1990). Typical complications such as vegetation, particle size and thermal shadowing (Ramsey and Christensen, 1993) are minimized upon examination of dunes. Actively saltating dunes contain little to no vegetation, are very well sorted and lack the thermal shadows that arise from rocky terrain. The primary focus of this work was to use the Kelso Dunes as a test location for an accuracy analysis of temperature/emissivity separation and linear unmixing algorithms. Accurate determination of ground temperature and component discrimination will become key products of future ASTER data.

A decorrelation stretch of the TIMS image showed clear color variations within the active dunes. Samples collected from these color units were analyzed for mineralogy, grain size, and separated into endmembers. This analysis not only revealed that the dunes contained significant mineralogic variation (Fig. 1), but were more immature (low quartz percentage) than previously reported (Sharp, 1966; Yeend, et al., 1984). Unmixing of the TIMS data using the primary mineral endmembers produced unique variations within the dunes and may indicate near, rather than far, source locales for the dunes.

The Kelso Dunes lie in the eastern Mojave Desert, California approximately 95 km west of the Colorado River. The primary dune field is contained within a topographic basin bounded by the Providence, Granite, Bristol and Kelso Mountains to the east, south, west and north, respectively. The dune field rests upon the alluvial fans which extend from the Providence and Granite Mountains, with the active region marked by three northeast trending linear ridges. Although active, the dunes appear to lie at an opposing regional wind boundary which produces little net movement of the crests (Sharp, 1966). Previous studies have estimated the dunes range from 70% (Sharp, 1966) to 90% (Paisley, et al., 1991) quartz mainly derived from a source 40 km to the west. The dune field is assumed to have formed in a much more arid climate than present, with the age of the deposit estimated at greater than 100,000 years (Yeend, et al., 1984).

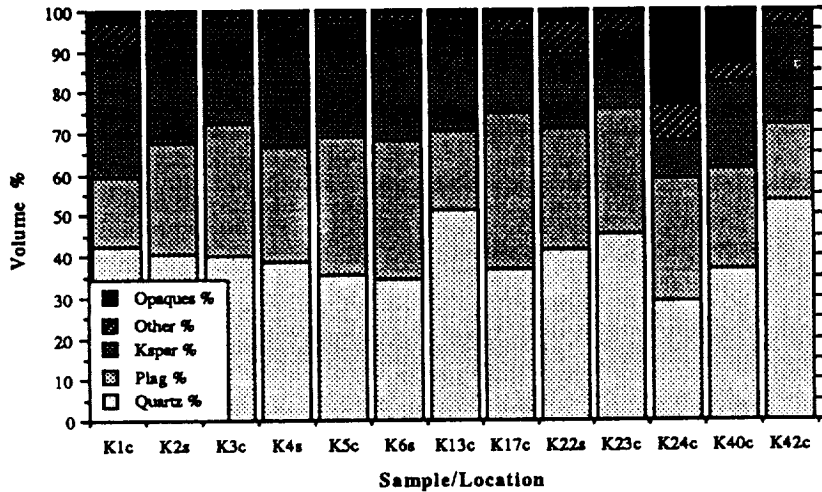


Figure 1. Mineral percentages derived from point-counts of thirteen sand samples. Sample numbers represent the collection site with a 'c' or 's' extension indicating a dune crest or swale. Samples K1c through K6s were collected from the same color unit and analyzed to verify the accuracy of the point-counting technique (note the similarity of the percentages). Samples K13c through K42c were collected along a 9.5 km N-S traverse through the most active region of the dune field (note the variation when compared to the first six samples). Also significant is the low average quartz percentage (40.4%).

## 2. SAMPLE ANALYSES

Forty-eight bulk samples were collected along a 9.5 km N-S traverse. These samples represented different image color units as well as position on the dune (crest vs. swale). Thirteen of the forty-eight bulk samples were chosen for detailed analyses to determine modal abundances. Six of these were from a small, mineralogically similar

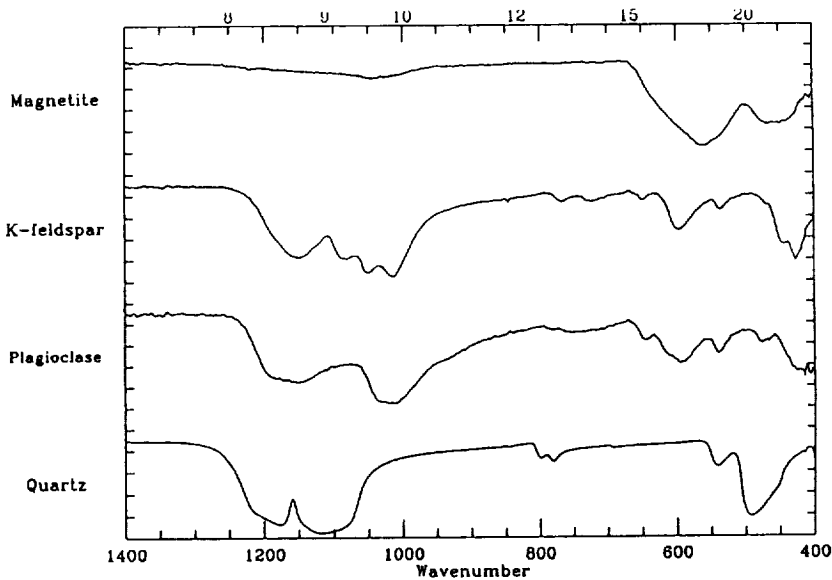


Figure 2. Laboratory emission spectra of the four endmembers - quartz, plagioclase, K-feldspar and magnetite (Avg. grain diameter = 500 - 710  $\mu\text{m}$ ). Minerals were separated from bulk samples using magnetic and heavy liquid separation techniques.

region and acted as a check on the consistency of the laboratory analysis. The bulk sand was split into 20 g samples (Cadle, 1955) from which thin sections and laboratory emission spectra were obtained (Christensen and Harrison, 1992). Over 200 grains per sample were counted to determine mineralogy and particle diameters (Jones, 1987). Samples K13c - K42c show clear mineralogic variations throughout the dune field (Fig. 1). These variations appear real based upon: (1) the color variations in the TIMS image; (2) the differences in the laboratory emission spectra; and (3) the similar point count results from samples K1c - K6s. Certain samples, collected from low-lying areas, contained appreciable amounts of clay. The clay component, separated from the sand using a Na-pyrophosphate dispersant, was analyzed by X-ray diffraction and found to be primarily montmorillonite. Finally, approximately 4 g of the dominant mineralogic components were separated using heavy liquid (Na polytungstate) and magnetic separation. While tedious, this separation insured the use of the correct endmembers for the dunes. Because the spectrum of plagioclase, for example, can vary dramatically as a function of An number, separation is preferred over the use of library spectra. The spectra of these endmember minerals (Fig. 2) were used as inputs into the unmixing algorithm for both the lab and image spectra.

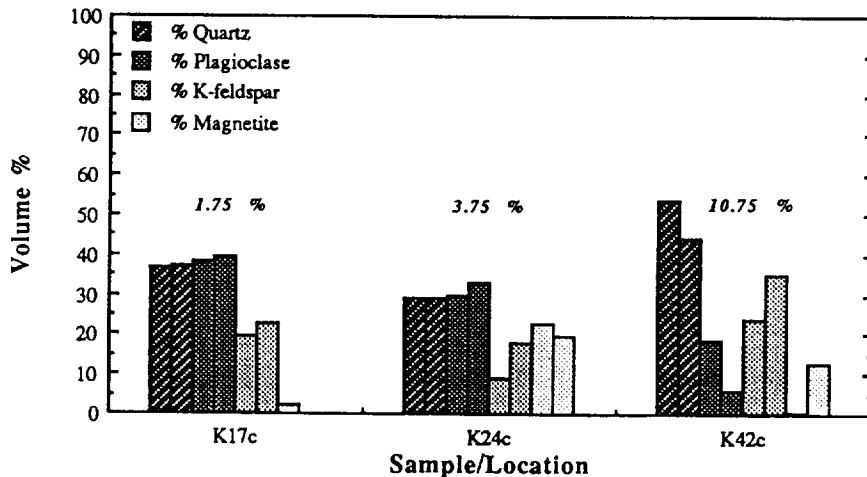


Figure 3. Comparison of endmember percentages derived from point counts (first bar) and the unmixing model (second bar). The three samples show the best, average and worst case error.

### 3. KELSO DUNES IMAGE ANALYSIS

Thermal Infrared Multispectral Scanner (TIMS) data for the Kelso region of the Mojave Desert were acquired in September 7, 1984. Ground resolution at nadir was approximately 17 m/pixel. The original flight line extends north from the dunes to the southernmost Cima basalt flows (Barbera, 1989). The data were calibrated and geometrically corrected for the scan angle of the instrument. Atmospheric path radiance was removed using LOWTRAN7 with the standard midlatitude summer model. The calibrated radiance images were then converted to six emissivity and one brightness temperature image (Realmuto, 1990) using a maximum assumed emissivity of 0.973 (derived from the average of all laboratory spectra). The spectra of the mineralogic endmembers convolved with the TIMS filter functions resulted in 6-point spectra that were used as inputs into the unmixing model. Mineral percentage images show very high concentrations of feldspar within the dunes as well as on alluvial surfaces extending from the immediate mountain ranges. This relation, coupled with the lack of feldspar being introduced from the previously assumed western source, indicates this mineral is

locally derived. By similar reasoning, the magnetite and other mafic minerals seem to be the direct result of weathering of amphibole rich metasediments in the Granite Mountains. While a certain percentage of the quartz within the dunes is likely derived locally, it appears, based on a higher concentration to the northwest, that some amount may come from the western source some 40 km away.

#### 4. RESULTS

This study represents a rigorous attempt to quantify and validate the linear mixing assumption of thermal emission spectra for a real geologic surface. It also is one of the more detailed laboratory studies of the Kelso sand mineralogy. The sum of both provided an excellent validation of mineralogic retrieval algorithms to remotely acquired data. Model-derived endmembers percentages agree to within an average of 5.4% of the point count figures. The error range varied from 1.75% (K17c) to 10.75% (K42c) (Fig. 3). The general agreement between the petrographic and spectral analyses is dramatic considering the time difference between image and sample collection, as well as the scale difference between image and lab samples. Applied to the TIMS data, the linear model reveals a much less mature dune mineralogy with a more local source for the sand than previously reported. Results of this study further the work of Ramsey and Christensen (1993) and indicate both the validity and power of the linear model especially when applied to thermal infrared image analysis.

#### 5. REFERENCES

- Barbera, P.W., 1989, *Geology of the Kelso-Baker Region, Mojave Desert, California using thermal infrared multispectral scanner data*, M.S. Thesis, Arizona State University, 198 p.
- Cadle, R.D., 1955, *Particle Size Determination*, Interscience Publishers, New York, N.Y., pp. 57.
- Christensen, P.R. and S.T. Harrison, 1992, "Thermal-Infrared Emission Spectroscopy of Natural Surfaces: Application to Desert Varnish Coatings on Rocks", submitted to *J. Geophys. Res.*
- Gillespie, A.R., M.O. Smith, J.B. Adams and S.C. Willis, 1990, "Spectral Mixture Analysis of Multispectral Thermal Infrared Images", in *Abbott, E.A. (Ed.), Proc. of the Second TIMS Workshop, JPL Pub. 90-55*, JPL, Pasadena, Calif., pp. 57-74.
- Jones, M.P., 1987, *Applied Mineralogy: A Quantitative Approach*, Graham and Trotman, Norwell, Mass., pp. 24, 74-75, 177.
- Paisley, E.C.I., N. Lancaster, L.R. Gaddis, and R. Greeley, 1991, "Discrimination of Active and Inactive Sand from Remote Sensing: Kelso Dunes, Mojave Desert, California", *Remote Sens. Environ.*, vol. 37, pp. 153-166.
- Ramsey, M.S. and P.R. Christensen, 1992, "The Linear 'Un-mixing' of Laboratory Infrared Spectra: Implications for the Thermal Emission Spectrometer (TES) Experiment, Mars Observer", *Lunar and Planet. Sci. XXIII*, pp. 1127-1128.
- Ramsey, M.S. and P.R. Christensen, 1993, "Ejecta Distribution at Meteor Crater, Arizona, Derived from Thermal Infrared Multispectral Scanner (TIMS) Data", to be submitted to *J. Geophys. Res.*
- Realmutto, V.J., 1990, "Separating the Effects of Temperature and Emissivity: Emissivity Spectrum Normalization", in *Abbott, E.A. (Ed.), Proc. of the Second TIMS Workshop, JPL Pub. 90-55*, JPL, Pasadena, Calif., pp. 26-30.
- Sharp, R.P., 1966, "Kelso Dunes, Mojave Desert, California", *Geol. Soc. Am. Bull.*, vol. 77, pp. 1045-1074.
- Yeend, W., J.C. Dohrenwend, R.S.U. Smith, R. Goldfarb, R.W. Simpson, Jr., and S.R. Munts, 1984, "Mineral Resources and Mineral Resource Potential of the Kelso Dunes Wilderness Study Area (CDCA-250), San Bernadino County, California", *U.S. Geol. Survey, Open File Report 84-647*, Washington D.C., 19 p.

## REMOTE IDENTIFICATION OF A GRAVEL LADEN PLEISTOCENE RIVER BED

Douglas E. Scholen

USDA Forest Service  
Southern Regional Office  
Engineering Unit  
1720 Peachtree Road  
Atlanta, Georgia 30367

### 1. INTRODUCTION

The abundance of gravel deposits is as well known in certain areas across the Gulf of Mexico coastal plain, including lands within several National Forests. These Pleistocene gravels were deposited following periods of glacial buildup when ocean levels were down and the main river channels had cut deep gorges, leaving the subsidiary streams with increased gradients to reach the main channels. During the warm interglacial periods that followed each glaciation, melting ice brought heavy rainfall and torrents of runoff carrying huge sediment loads that separated into gravel banks below these steeper reaches where abraiding streams developed. As the oceans rose again, filling in the main channels, these abraiding areas were gradually flattened and covered over by progressively finer material. Older terraces were uplifted by tectonic movements associated with the Gulf Coastal Plain, and the subsequent erosional processes gradually brought the gravels closer to the surface.

The study area is located on the Kisatchie National Forest, in central Louisiana, near Alexandria. Details of the full study have been discussed elsewhere (Scholen et al., 1991). The nearest source of chert is in the Ouachita Mountains located to the northeast. The Ouachita River flows south, out of these mountains, and in Pleistocene times probably carried these chert gravels into the vicinity of the present day Little River Basin which lies along the eastern boundary of the National Forest.

Current day drainages cross the National Forest from west to east, emptying into the Little River on the east side. However, a north-south oriented ridge of hills along the west side of the Forest appears to be a recent uplift associated with the hinge line of the Mississippi River depositional basin further to the east, and 800,000 years ago, when these gravels were first deposited during the Williana interglacial period, the streams probably flowed east to west, from the Little River basin to the Red River basin on the west side of the Forest.

Within the National Forest land north of Alexandria, along Fish Creek, and east and west of an area known as Breezy Hill, exist several small, worked out gravel pits on privately owned blocks of land, formerly used by the state and county road departments. The pattern presented by these pits give the impression of a series of north-south drainages lacing through the Forest, probable tributaries to Fish Creek which flows south of east from the west side of the Forest to empty into the Little River. Because of this predominant north-south pattern, no consideration was given to areas between these drainages during early gravel exploration efforts.

### 2. IMAGE ACQUISITION

The initial imagery, obtained for the U.S. Forest Service during the predawn hours of early October in 1983 by the NASA, Stennis Space Center, Earth Resources laboratory, was acquired with the Thermal Infrared Multispectral

Scanner (TIMS) from the Lear 23 at an altitude of 12,000 meters above terrain, and provided data with 30 meter pixels and a swath width of approximately 18.7 kilometers. This time had been a particularly hot and dry period, and provided bone dry ground conditions as well as maximum outflow of heat from the earth's surface into the cool night sky. These conditions are ideal for obtaining good imagery for gravel search.

The 6 bands of data obtained from the TIMS operation are in digital format. This format provides a relative measure of the emissivity from the ground surface soil minerals at each of the 6 wave lengths within the mid-infrared range, and makes it possible to plot a spectral signature for each pixel.

### **3. SPECTRAL PROPERTIES**

The materials properties that provide differences between spectral signatures of gravel deposits and deposits of other, finer grained materials are the energy absorption of the quartz molecule in TIMS band 3, the fraction of silt and clay in the material, and the thermal inertia of the material.

The energy absorption is caused by the stretching of the molecular bonds between the oxygen and silicon atoms that occurs in making up the SiO<sub>2</sub> molecule and its linkages. In order to maintain this configuration, the molecule must absorb energy from outside itself in the wave lengths associated with the TIMS band 3. This provides the striking signature associated with quartz. Gravel, and clean, dry, coarse grains provide the strongest signatures. Silt, impurities from clay minerals or other rock minerals, all tend to produce photon scattering which dilutes the signature.

The coarse nature of sand deposited with gravel deposits is a result of the velocity of flow in the channel. Finer particles resist settlement until still water is reached, preventing the fine and coarse materials from intermingling. Coarse sand and gravel settle out in moving water. This separation is assisted by lateral movements in the river channel. A river carrying a coarse grained load will develop a straight, shallow channel, but will change to a meandering, deep channel when the bedload becomes silt and clay leaving much of the coarse grained deposit intact.

The predominance of coarse sands found associated with gravel deposits identified by the TIMS gravel signatures indicates that these signatures are characteristic of coarse grained quartz deposits, and conversely, that the strong energy absorption in TIMS band 3 is maximized by coarse grained quartz. Thus a marked decrease in band 3 emission (and correspondingly greater dip in the signature at this point) can be expected for the coarser sized sands and gravels, as compared to the finer grained silts.

### **4. THERMAL INERTIA**

The thermal inertia of materials provides for striking contrasts in surface temperatures. Thermal inertia expresses the resistance of a material to temperature change. Materials of high thermal inertia change temperature only very slowly, lagging behind changes in adjacent materials with low thermal inertia. A deposit of sand and gravel for example has a higher thermal inertia than a deposit of sand. This difference is most apparent in TIMS band 3, at 9.3 microns wavelength due to the energy absorption by Si-O molecular bonding, which maintains a low temperature at this wavelength while the sandy gravel mass absorbs heat from solar radiation.

The combination of maximum summer heating together with early morning cooling provides for a unique effect associated with materials of high thermal inertia. The temperature rises high in the low thermal inertia sand exposed over the summer months to the hot sun warming the surface. The higher thermal inertia gravel absorbs more heat than the sand but resists temperature change, warming more slowly, and in the predawn hours of early Fall, surface cooling

produces a lower surface temperature over the gravel body than over the sand deposits, when viewed in TIMS band 3. Gravel/sand deposits always show cooler in the TIMS band 3 imagery than adjacent nongravel/sand deposits, although warmer than the damp bottom land.

## 5. IMAGE PROCESSING

Imagery is processed on a 486 PC with 650MB hard drive and 90 MB Bernoulli, using ERDAS 7.5 software and ARC/INFO. The image for this study was prepared from the 1983 TIMS imagery. A subset including the area of concern was corrected to uniform pixel size by multiplying raw DN's by the  $\text{Cos}^4$  of the angle from Nadir. The scene was rectified and georeferenced, and a road map from the GIS file was superimposed to assist in the geographic location of gravel signature. Bands 2,3 and 4 were displayed in blue, green and red respectively. The gravel signature was developed using the ERDAS SEED software. Using the cursor, single pixel seeds were located which show the maximum difference between TIMS bands 3 and 4 in the cooler areas of the scene, and these were alarmed to the entire scene. Several seed pixels were located due to the range in temperatures across the gravel deposits. The resulting gravel signature is actually a composite. Seed pixels can be located by searching along the edges of the darker areas of the image. The lower DN's on gravel deposits in band 3, caused by the greater absorption of radiation, results in a moderately dark image. While drainage bottoms are generally dark, the signature of silt is relatively flat. The brightest areas are ridge tops, unless gravel is present on the ridge to reduce the brightness. The difference between DN's in bands 3 and 4 increases with increasing brightness. An open gravel pit will have a very large increase from band 3 to band 4.

## 6. DISCOVERY

During the image processing procedure associated with gravel deposit search, blocks of imagery are processed and studied for potential gravel signature. The area on the east side of the Forest, directly south of Fish Creek, was found to be obscured by clouds which formed during the overflight. To the north of this cloud cover, the processed raw image data indicated gravel signature in a nearly uniform east-west band, that appeared to be some kind of data anomaly. Initially, no attention was given to it. Subsequently, the image in this area was rectified to map coordinates, and it was discovered that the band of gravel signature actually trends north of west across the Forest for over 14 kilometers, and crosses the Fish Creek drainage at a narrow angle near the mid point of the signature band. The signature band thus runs nearly at 90 degrees to the north-south tributaries to Fish Creek, and crosses a number of low north-south trending ridges lying between these tributary drainages.

Several of these ridges were already accessible to our drill rig on existing road tracks. On each of these where drilling was performed, shallow gravel deposits were found in the area where the gravel signature crossed the ridge. Following these successes, other less accessible ridges were accessed through brush, or by bulldozing a temporary access through light timber. In each of these areas investigated, gravel deposits were found in the locations indicated by the imagery, and work continues as other ridges become accessible. Thickness of the deposits varied from a meter up to nearly 10 meters. Overburden varied from 0 to 2 meters. Total volume of gravel in these deposits is estimated to exceed 500,000 cubic meters. The width of the 8 kilometer gravel run probably averages 60 meters, providing an indication of the size of the ancient river bed.

## 7. REFERENCES

Scholen, D.E., W.H. Clerke, and G.S. Burns, "Remote Spectral Identification of Surface Aggregates by Thermal Imaging Techniques: Progress Report". In International Society of Optical Engineers (SPIE), Vol. 1492 Earth and Atmospheric Remote Sensing, pp 359-369, 1991.



Figure 1. TMS 30 meter resolution image of the Breezy Hill area, Catahoula Ranger District, Kisatchie National Forest. The image has been partially rectified, and processed to highlight pixels with a quartz gravel signature, indicated by the pattern of black spots spread across the image. The gravel deposits lie on flat, current day ridges, along the former channel of a meandering, Pleistocene Age, river. The bright curved line extending from mid lower image to the upper right is Grant Parish Road 123. The bright north-south line at the right is US165, north of Alexandria, LA. The large bright spot near image center is a pond in the Fish Creek drainage, which crosses the parish road and flows slightly south of east, through the bright area. Fish Creek to the west is obscured by clouds.



1. Report No. 93-26, vol. 2		2. Government Accession No.		3. Recipient's Catalog No.	
4. Title and Subtitle Summaries of the Fourth Annual JPL Airborne Geoscience Workshop, October 25-29, 1993 Volume 2. TIMS Workshop				5. Report Date October 25, 1993	
				6. Performing Organization Code	
7. Author(s) Vincent J. Realmuto, editor				8. Performing Organization Report No.	
9. Performing Organization Name and Address JET PROPULSION LABORATORY California Institute of Technology 4800 Oak Grove Drive Pasadena, California 91109				10. Work Unit No.	
				11. Contract or Grant No. NAS7-918	
				13. Type of Report and Period Covered JPL Publication	
12. Sponsoring Agency Name and Address NATIONAL AERONAUTICS AND SPACE ADMINISTRATION Washington, D.C. 20546				14. Sponsoring Agency Code RF4 BP-465-66-00-01-00	
15. Supplementary Notes					
16. Abstract This publication contains the summaries for the Fourth Annual JPL Airborne Geoscience Workshop, held in Washington, D.C. on October 25-29, 1993. The main workshop is divided into three smaller workshops as follows: <ul style="list-style-type: none"> <li>o The Airborne Visible/Infrared Imaging Spectrometer (AVIRIS) workshop, on October 25-26. The summaries for this workshop appear in Volume 1.</li> <li>o The Thermal Infrared Multispectral Scanner (TIMS) workshop, on October 27. The summaries for this workshop appear in Volume 2.</li> <li>o The Airborne Synthetic Aperture Radar (AIRSAR) workshop, on October 28-29. The summaries for this workshop appear in Volume 3.</li> </ul>					
17. Key Words (Selected by Author(s)) Environmental biology Instrumentation and photography Geology and mineralogy Snow, ice, permafrost			18. Distribution Statement Unclassified; unlimited		
19. Security Classif. (of this report) Unclassified		20. Security Classif. (of this page) Unclassified		21. No. of Pages 28	22. Price

